Journal of *Marine Science and Engineering*

MDPI

Article

Barcelona Coastal Monitoring with the "Patí a Vela", a Traditional Sailboat Turned into an Oceanographic Platform

Inmaculada Ortigosa [1,*], Raul Bardaji [2], Albert Carbonell [3], Oriol Carrasco [4], Marcella Castells-Sanabra [1], Rafel Figuerola [3], Nina Hoareau [4], Jordi Mateu [1], Jaume Piera [4], Joan Puigdefabregas [5], Joaquín Salvador [4], Carine Simon [4], Ignasi Vallès-Casanova [4] and Josep L. Pelegrí [4,*]

1 Departament de Ciència i Enginyeria Nàutica, Universitat Politècnica de Catalunya, 08003 Barcelona, Spain; marcella.castells@upc.edu (M.C.-S.); jordi.mateu@upc.edu (J.M.)
2 Marine Technology Unit, Department of European Multidisciplinary Seafloor and Water Column Observatories, CSIC, 08003 Barcelona, Spain; bardaji@utm.csic.es
3 Club Patí de Vela de Barcelona, 08003 Barcelona, Spain; albert.ca89@gmail.com (A.C.); info@pativelabarcelona.com (R.F.)
4 Departament d'Oceanografía Física i Tecnològica, Institut de Cienciès del Mar, CSIC, 08003 Barcelona, Spain; carrasco@icm.csic.es (O.C.); nhoareau@icm.csic.es (N.H.); jpiera@icm.csic.es (J.P.); jsalvador@icm.csic.es (J.S.); csimon@icm.csic.es (C.S.); valles@icm.csic.es (I.V.-C.)
5 Departament de Física, Universitat de les Illes Balears, 07122 Palma de Mallorca, Spain; joan.puigdefabregas@uib.cat
* Correspondence: inmaculada.ortigosa@upc.edu (I.O.); pelegri@icm.csic.es (J.L.P.); Tel.: +34-934010873 (I.O.)

Abstract: Shelf waters near large cities, such as Barcelona, are affected not only by meteorological episodes but also by anthropogenic influence. Scientists usually use data from on-site coastal platforms to analyze and understand these complex water ecosystems because remote sensing satellites have low spatiotemporal resolution and do not provide reliable data so close to the coast. However, platforms with conventional oceanographic instrumentation are expensive to install and maintain. This study presents the scientific adaptation and initial measurements from a "patí a vela", which is a very popular unipersonal catamaran in Barcelona. This versatile sailing vessel has been adapted to contain several low-cost sensors and instruments to measure water properties. Here, we describe the setup of a multi-parameter prototype, and then focus on results obtained using a low-cost temperature profiler. First, the temperature data are compared and validated with another conventional oceanographic instrument used in monthly oceanographic cruises. Then, field measurements between July and November 2021 are used to explore the relationship between air and water temperature in the Barcelona coastal area, showing the seasonal evolution of the temperature profile. We conclude that citizen sampling from fully sustainable sailing boats may turn into an effective strategy to monitor the urban coastal waters.

Keywords: scientific sailing boat; low-cost sensors; temperature-depth profiler; citizen science

Citation: Ortigosa, I.; Bardaji, R.; Carbonell, A.; Carrasco, O.; Castells-Sanabra, M.; Figuerola, R.; Hoareau, N.; Mateu, J.; Piera, J.; Puigdefabregas, J.; et al. Barcelona Coastal Monitoring with the "Patí a Vela", a Traditional Sailboat Turned into an Oceanographic Platform. *J. Mar. Sci. Eng.* **2022**, *10*, 591. https://doi.org/10.3390/jmse10050591

Academic Editors: Georgy I. Shapiro and Mikhail Emelianov

Received: 31 January 2022
Accepted: 20 April 2022
Published: 27 April 2022

1. Introduction

The United Nations adopted, in 2015, the 2030 Agenda for Sustainable Development, a blueprint towards global welfare for current and future generations. Within this agenda, sustainable growth in the marine and maritime sectors requires the development of effective tools, in terms of decreased uncertainty and low cost, for seawater quality monitoring.

Coastal marine environments are particularly vulnerable to both climate change and global change. The coastline is indeed susceptible to major impacts associated with anthropogenic climate change, particularly the rising sea level and the more frequent extreme meteorological events [1]. It is also affected by increased contaminants and degraded benthic habitats, with far-reaching implications for marine ecosystems and human health and welfare [2]. However, coastal waters are under sampled both in time and space [3] due

to the difficulty of setting oceanographic platforms that can carry out continuous sampling away from the coastline and the limited accuracy and spatiotemporal resolution of satellites in the shelf waters. In contrast, in recent years, there have appeared different innovative ways of sampling coastal waters that take advantage of the number of participants engaged in nautical recreation sports [4–7].

Barcelona, with a population of over 3.3 million people in its metropolitan area, has a high impact on its coastal marine system. This, in turn, causes Barcelona citizens to become negatively affected by unhealthy marine ecosystems, impacting other economic areas such as local fisheries and tourism. With heavy rain and high seas, stormy episodes are remarkable examples of this two-way interaction. They lead to high-polluted coastal waters (because of water runoff from the city) and beach-width reduction, which affect the coastal environment and shoreline at different time scales.

Given its social and ecological relevance, it is of fundamental importance to understand and preserve the marine environment of Barcelona. The first condition to understand this environment is to monitor its spatiotemporal variations. Despite the apparently easy access to the marine environment in Barcelona, coastal monitoring is limited by the high cost and limited flexibility of classical oceanography. Apart from the water quality control carried out in summer (bathing water status) and a daily examination of the surface temperature carried out by the Catalan Water Agency [8,9], the only systematic year-long offshore sampling has been along a line normal to the Somorrostro Beach (PUDEM line), carried out since 2002 [10,11]. These data are available from the Institut de Ciències del Mar (ICM) [12] and have led to several reports and scientific publications [13–15].

In order to improve the sampling frequency and spatial coverage, we propose a local strategy for monitoring the Barcelona inner-shelf waters with the participation of sailors that use the patí a vela (PV), a recreational sailing boat widely used in Catalonia. Nowadays, the PV fleet is also found far beyond Catalonia, with sailing boats in Valencia and Andalusia, and also reaching the French, Belgian and Dutch coasts.

According to the International Patin Sailing Association (ADIPAV) data, more than 200 PV sailing boats could be directly involved with citizen sampling near Barcelona. If part of these recreational boats were equipped with an oceanographic low-cost-sensors platform, the sampling capacity of environmental indicators in Barcelona and nearby coastal waters would be significantly enhanced. In this article, we first explain how the PV is adapted to become an oceanographic sampling platform and then illustrate its potential for monitoring the coastal waters by presenting temperature data gathered in the summer and fall of 2021.

2. Patí Científic Project

The project "Development of a citizen monitoring program for the Barcelona coastal waters: the Scientific Patí a Vela (PATI CIENTIFIC)" is a collaborative initiative of the ICM, the Club Patí de Vela de Barcelona (CPVB), and the Facultat de Nàutica de Barcelona, with funding from the Barcelona City Council. The main objective of PATI CIENTIFIC is to develop an inclusive and transformative low-cost resource that can effectively help monitor the coastal waters. This is undertaken by designing, constructing and testing two main sampling devices: a multi-parametric box adapted on-board the PV, which becomes a multi-platform instrument to sample the surface waters while the PV sails, and a temperature-depth profiler, which can be used in specific sites to observe the thermal structure of the water column. In this way, the PV is easily converted into a scientific PV (SPV); a sailboat ready to provide valuable environmental information about the nearby coastal ocean.

All data collected with the SPV are freely available thanks to the development of a Web portal (https://paticientific.org/ (accessed on 13 April 2021) where data are incorporated and retrieved in the context of the philosophy of Open Science, hence promoting citizen engagement in scientific data collection and turning research into a process of social participation.

3. Materials and Equipment

3.1. Scientific Patí a Vela Description

A PV is a lightweight sailing catamaran, usually wooden and with a crew of only one person. It originated in Barcelona and nearby Badalona during the middle of the 20th century, as citizens wanted to bath in clean waters, away from the near-beach pollution that was largely caused by factories along the coastline. The standard design currently in use follows the original one designed by the Mongé brothers in 1943 [16,17]. The PVs' main peculiarities are that it does not have a rudder, keel or boom, so it goes into the water directly from the beach (Table 1).

Table 1. Main characteristics of the Scientific Patí de Vela.

LOA	Beam	Displacement (Hull)	Sail Area	Hull Type
5.60 m	1.60 m	89 kg	12.60 m^2	Catamaran

The PV is maneuvered by modifying the relative distance between the hull and sail pressure centers by simply displacing the crew along the deck (Figure 1). When the crew moves, so does the boat's gravity center, and the PV trim is consequently modified. The sail pressure center can be controlled by adjusting the tension in the sail.

Figure 1. Picture of an SPV while departing from the CPVB premises, near downtown Barcelona, with the ICM facilities at the back. The insets illustrate the steering control of the PV, reprinted/adapted with permission of Ref. [17]. 1974, Editorial Hispano Europea.

The PV turns into the SPV when adapted and equipped with an on-board multiparametric box, which contains a water pump, battery, electronics and a sensor box (Figure 2). The sensor box is modular, so that sensors can be easily incorporated into or removed from the box. We have tested temperature (PT1000), conductivity (pro K10), pH (LabGrade) and dissolved oxygen (ENV-40-DOC) sensors provided by Atlas Scientific (Long Island City, NY, 11101); although, only the temperature and conductivity sensors are used routinely for monitoring. The sensors are connected to a Smart Citizen kit, which contains a central data logger, developed by FabLab Barcelona (https://fablabbcn.org/ (accessed on 13 April 2022)). Two flexible tubes reach in and out from the sensor box, pumping surface water through the several sensors located inside the box and releasing it back to the sea. In this way, we can continuously sample the surface oceanographic variables, which can either be stored internally in the data logger or

transmitted with a smartphone. The overall cost of the multiparametric box with temperature and conductivity sensors is about EUR 550.

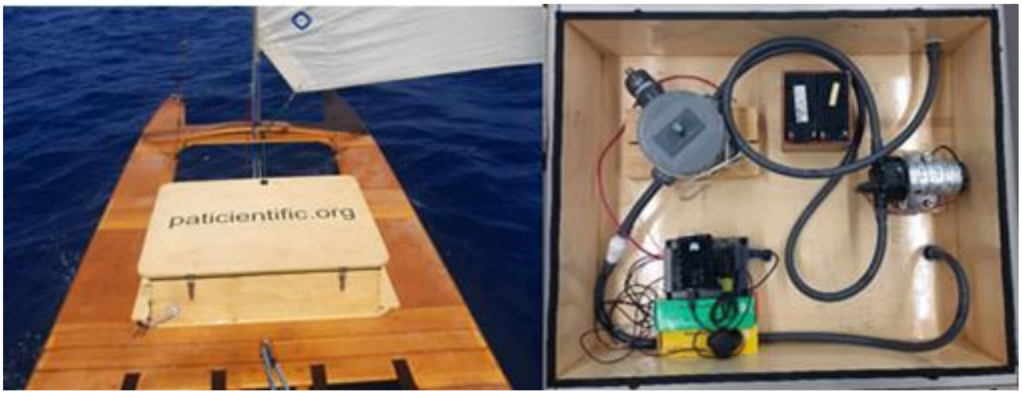

Figure 2. (**Left**) Removable on-board multiparametric box installed in a PV. (**Right**) Detail of the interior configuration of the removable on-board multiparametric box.

The on-board multiparametric box, which is placed between the second and third bench of the catamaran (Figure 2), modifies the displacement, gravity center and trim of the boat. If the skipper wants to maintain the direction of the boat, he/she has to sit closer to the stern than without the instrumented box installed onboard. However, these changes have little effect on the boat's stability, resistance and maneuverability. Ortigosa et al. [18] analyzed the effects of this prototype box on the hydrodynamics of the sailing boat, both numerically and at sea, and determined the best configuration that preserves the essential stability characteristics so that it does not interfere with the seakeeping performance of this recreational boat in the water.

Figure 3 illustrates the changes in sea-surface temperature (SST) and sea-surface salinity off downtown Barcelona as sampled with the multiparametric box on the SPV on 22 July 2021. The data, gathered in less than two hours, illustrate substantial temperature and salinity changes in relatively small distances, emphasizing the potential of the SPV to quickly sample the short-scale spatial variability.

3.2. SPV TD Instrument and Sensors

The SPV is also equipped with a hand-held open-source temperature-depth (TD) profiler that can be deployed down to depths of about 100 m and stores data on a uSD memory card. The low-cost sensors reduce the price of the entire setup by a factor of ten and open the possibility that several SPVs simultaneously sample the coastal waters, significantly improving the spatial and temporal monitoring. Further discussions in this article focus on the profiles obtained by this SPV TD profiler.

The TD profiler needs to be simple enough for use by sailors; additionally, it has to be small so that it does not interfere substantially with the center of gravity and maneuverability of the boat (Figure 4). The TD profiler consists of temperature and pressure sensors connected to an Arduino Pro Mini, with all electronics and sensors assembled in a waterproof housing made of commercial PVC components [19].

The sensors used are from Blue Robotics: the Celsius Fast Response temperature sensor with 0.1 °C accuracy that samples between −5 and 50 °C and has an operating depth range of 0–975 m; and the Bar30 pressure sensor with an accuracy of 200 mbar and operating range of 0–300 m. Connections are made with a custom-designed PCB, and activation is performed with an external magnetic switch. When the profiler is switched on, it starts recording data continuously at 1 Hz on a uSD memory card. The instrument is lowered by hand and has been tested down to 100 m depth. The overall cost for the components of this SPV TD is less than EUR 300.

Figure 3. (**Top**) Sea-surface temperature and (**bottom**) sea-surface salinity on 22 July 2021, along the navigation track of the SPV.

Figure 4. SPV TD aside the Sea & Sun CTD 48Mc probe; the respective lengths are approximately 20 cm and 45 cm long.

During the field campaign, the SPC sails to every study point, where the temperature vs. depth profile is recorded. As the PV has no electronics or navigation systems, the positioning is set using a smartphone. The procedure of recording the temperature profile at every point consists of the following steps: the boat is stopped in the desired location; the low-cost TD profiler is switched on and kept on the surface for 60 s to acclimatize the temperature sensor; the profiler is released until reaching the desired depth and then it is recovered and switched off.

3.3. SPV TD Sensors Validation

The open-source TD profiler was validated by comparison to data from a Sea & Sun 48Mc CTD, gathered down to 100 m in a station located in Estartit, along the Catalan coast and north of Barcelona. For the comparison, both datasets were first collocated in time, then interpolated at 1 Hz, and finally the temperature and pressure data were fitted with a linear regression. Figure 5 compares the temperature profiles from both instruments, and

Figure 6 presents the dispersion graphs for both sensors, with regression coefficients very close to one.

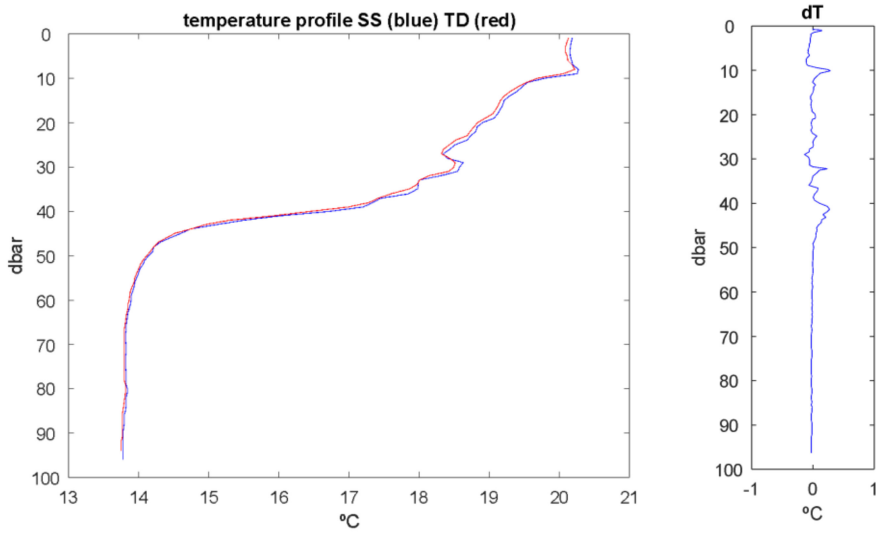

Figure 5. (**Left**) Temperature profiles obtained with the SPV TD profiler (red curve) and with the Sea & Sun CTD 48Mc (blue) and (**right**) their difference (CTD minus TD values).

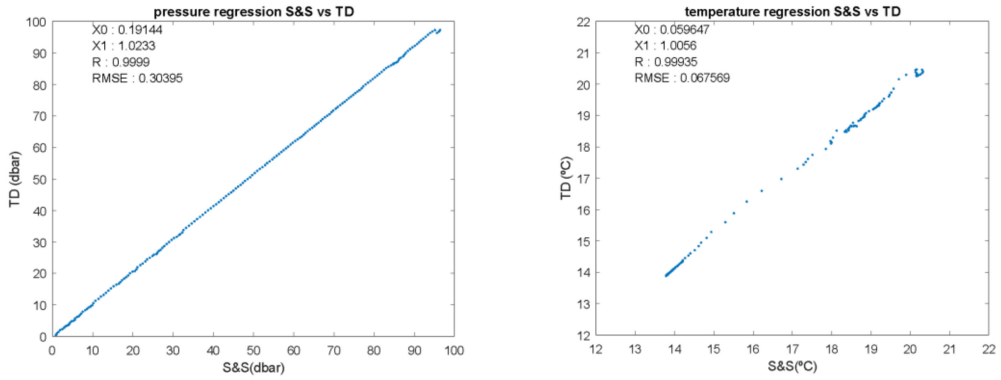

Figure 6. Regression plots for (**left**) pressure and (**right**) temperature between the PV TD and Sea & Sun CTD 48Mc probes.

The SPV TD produces a slightly smoother profile than the Sea & Sun CTD, which is consistent with a slightly slower response from the Celsius Fast Response temperature sensor. Nevertheless, the downcast temperature profiles match very well, with a global difference of -0.054 ± 0.055 °C, below the nominal resolution of both sensors. Note that in the deeper and more stable part of the profile (50 to 100 m) the difference is smaller (-0.024 ± 0.005 °C) while differences are larger in the upper 50 m of the profile (-0.080 ± 0.066 °C), possibly due to a slower response of the SPV TD or partly to turbulence generated by the Sea & Sun profiler, which was placed 1 m below the SPV TD.

3.4. Data Acquisition and Quality Control in the SPV Surveys

The data acquisition is quite simple and can be carried out by non-specialized sailors. Once the SPV arrives at the study point, the TD profiler is switched on, held for one minute at the sea surface for sensor stabilization, and lowered with a rope at a rate of about 0.5 m s^{-1} down to the maximum desired depth. Once the profiler is recovered onboard, it is switched off and the SPV sails to the next sampling point. As the ship has no electronic navigation, positioning is recorded on a mobile phone and stored in an independent dataset to be merged with oceanographic data in the post-processing steps.

A specific quality control is applied to the raw TD measurements, adapted from common oceanographic CTD data processing [20,21] and from specific observations during the SPV cruise. During the data processing, a quality flag value is assigned at each measurement (Table 2).

Table 2. Quality control flag values applied during the data processing.

Flag Value	Definition Term	Abbreviated Term
0	No quality control procedures have been applied to the data value. This is the initial status for all data values entering the working archive.	No quality control
1	Good quality data value that is not part of any identified malfunction of the instrument and has been verified as consistent with real phenomena during the quality control process.	Good
2	This value has been derived by interpolation from other values in the data object.	Interpolated
3	Data value is recognized as unusual during quality control, possibly inconsistent with real phenomena.	Suspect
4	An obviously erroneous data value	Bad
9	The data value is missing.	Missing

Data are considered "bad" (flag = 4) if one of the following occurs: (i) data correspond to the first 10 s after switching on, as the temperature sensor needs times to stabilize; (ii) data are located between the sea surface and 1 m depth; (iii) a temperature value is too far from the mean nearby values, and the criteria chosen being that the difference in data with the mean value is greater than four times the standard deviation. Data are flagged as "suspect" (flag = 3) if one of the following happens: (i) the downcast velocity is less than 0.2 m/s, potentially leading to multiple values at one single depth; (ii) we observe a loop in the profile due to the movement of the boat. Finally, the good data (flag = 1) are averaged every 0.2 m in order to create a temperature profile with regular sampling. When data are missing, an interpolation is applied and the data are flagged (flag = 2). Figure 7 shows a sample dataset in a station after applying the quality control procedure.

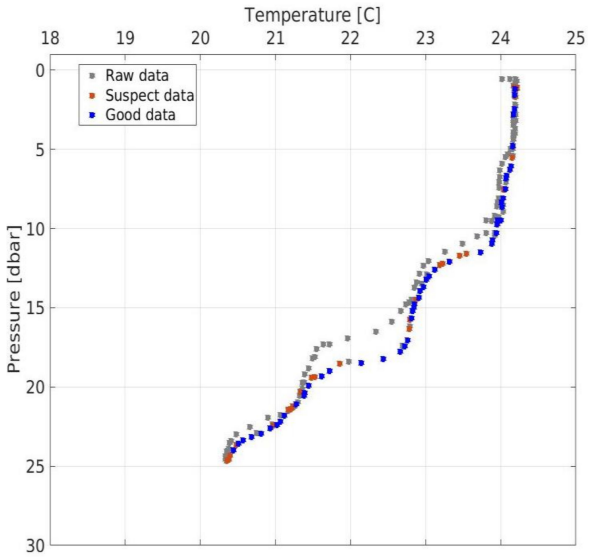

Figure 7. TD profile after applying the data quality procedure (station TD5, 1 October 2021). Both the downcast (colored points) and upcast (grey points) profiles are shown. Blue dots represent the good data (flag = 1) while orange dots correspond to data flagged as suspect data (flag = 3).

4. Methods

4.1. Study Area

The coastal zone studied is in front of the Somorrostro beach, near downtown Barcelona. This area is also close to the Port Olympic, a Marina with remarkable yachting activity during the summer season (Figure 8). Most of the Barcelona coastline becomes a fairly crowded beach during summer, and the study area is also affected by runoff water from the city collected by two of the city outfalls. In the case of high rainfall, the city outfalls may discharge untreated street water into the sea [15]. Therefore, a strong anthropogenic pressure affects the natural conditions of the study area.

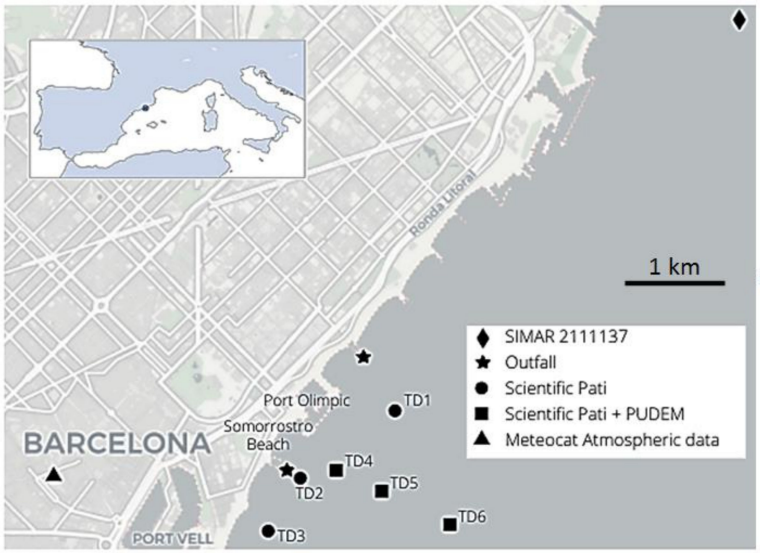

Figure 8. Study area off Barcelona with the location of the TD, wave and meteorological stations. Stations TD4, TD5 and TD6 coincide with three of the stations of the monthly PUDEM monitoring [15].

The area of study is the inner-shelf in front of the city of Barcelona, in the NW Mediterranean Sea (Figure 8). This is an area where the atmosphere–ocean interaction modifies the water masses throughout the year, with a mean monthly range of 14 °C. From spring to autumn, a seasonal thermocline is formed; in winter this thermocline vanishes and the water column turns homogeneous [15]. The zone is characterized by a predominant current from the northeast that drives the relatively low-density shelf water [22].

Six measurement stations (TD1 to TD6) were used to assess the complexity of the area, which goes from 41.3749° N to 41.3856° N and from 2.1951° E to 2.2162° E (Table 3). Station TD1 allows the study of the area located east of Port Olympic. This point receives the direct flow of water, which enters the study zone from the northeast. It may also influence one of the outfall points that can be seen on the map. TD2 is located in front of one of the water discharge points of the city and in front of the Port Olympic mouth. TD2 and TD3 are the points closer to the beach.

TD4, TD5 and TD6 are stations along a line normal to shore, which permit studying the evolution of the vertical temperature structure with increasing depth and distance to shore. These three points coincide with the study points during the oceanographic PUDEM cruises. In Figure 8, we also indicate the location of a SIMAR model point, where wave period and height are available from Puertos del Estado [23], and a nearby city meteorological station, where wind velocity, air temperature and solar radiation are available from the Catalan Meteorological Service [24].

Table 3. Position of the six measurement stations, showing the maximum depth (Mdepth) reached by the TD profiler. The bottom depth in stations TD5 and TD6 is about 30 and 40 m, respectively.

	Latitude (N)	Longitude (E)	Mdepth (m)
TD1	41.3856°	2.2099°	23
TD2	41.3798°	2.1986°	12
TD3	41.3749°	2.1951°	11
TD4	41.3806°	2.2029°	20
TD5	41.3785°	2.2084°	28
TD6	41.3757°	2.2162°	28

4.2. Period of Study

For real-time coastal ocean monitoring, field campaigns with the SPV were carried out in the study area in July, August, September, October and November 2021, for a total of 15 days (Table 4). This represents nearly one weekly cruise, designed to record the temperature profile in depth using the low-cost temperature profiler synchronized with meteorological data. Data are missing for some weeks, as the SPV requires some minimum wind conditions for sailing.

Table 4. Dates between July and November 2021 when TD data were acquired with the SPV.

Date	TD1	TD2	TD3	TD4	TD5	TD6
28 July	X	X	X			
3 August	X	X	X			
17 August	X	X	X			
31 August				X	X	X
6 September				X	X	X
17 September	X	X	X	X	X	X
21 September	X	X	X	X	X	X
28 September	X	X	X	X	X	X
1 October	X	X	X	X	X	X
5 October	X	X	X			
7 October	X	X	X	X	X	X
18 October	X	X	X			
28 October	X	X	X	X	X	X
8 November	X	X	X	X	X	X
18 November				X	X	X

Not every field campaign obtained data at all stations. If the meteorological conditions changed during the field campaign, caused by an extreme rise or fall in the wind, it may not have been possible to complete the sampling in all stations.

4.3. Other Datasets

We use SST data from the WST-non time-critical Sentinel-3 satellite products [25], available from the Puertos del Estado web platform (www.puertos.es (accessed on 20 November 2021)). This satellite delivers daily data at a spatial resolution of 1 km (0.3 °C precision when cloudiness is below 20%). A single SST value is derived along the swath of the satellite, using the best-performing sensor algorithms and supporting data field. Only data flagged as being of "excellent

quality" are used. This causes that only 25 satellite SST values are available for our 4-month study period.

Hourly wave period and height data come from the coastal model SIMAR [23], developed by Puertos del Estado (www.puertos.es (accessed on 20 November 2021)). The closest point to the sampling area used in this study is SIMAR 2111137 (2.25°E, 41.42°N). Hourly observations of wind velocity, air temperature and solar radiation come from the Catalan Meteorological Service [24], concretely from the station located at 41.38° N 2.17° E, near downtown Barcelona. Daily averages of each variable are calculated, except for the maximum radiation and accumulated daily rainfall.

Meteorological and wave data during the period of our study are shown in Figure 9. Figure 9b shows the squared wind speed, as an indicator of the wind energy available to mix the water column, either in the form of waves or as turbulence that can increase the depth of the surface mixed layer. This figure reveals that wind remains relatively low during the summer months (July, August and early September) and that there are four events where the values exceed 40 m^2 s^{-2}: 22–23 September, 4 October, 20 October and particularly 10–11 November, when values exceeded 120 m^2 s^{-2}. Figure 9d presents the wave energy per unit length (proportional to the squared significant wave height) for this same period. This figure suggests a good correspondence between intensified winds and increased waves, indicating that most of the wave episodes are locally generated.

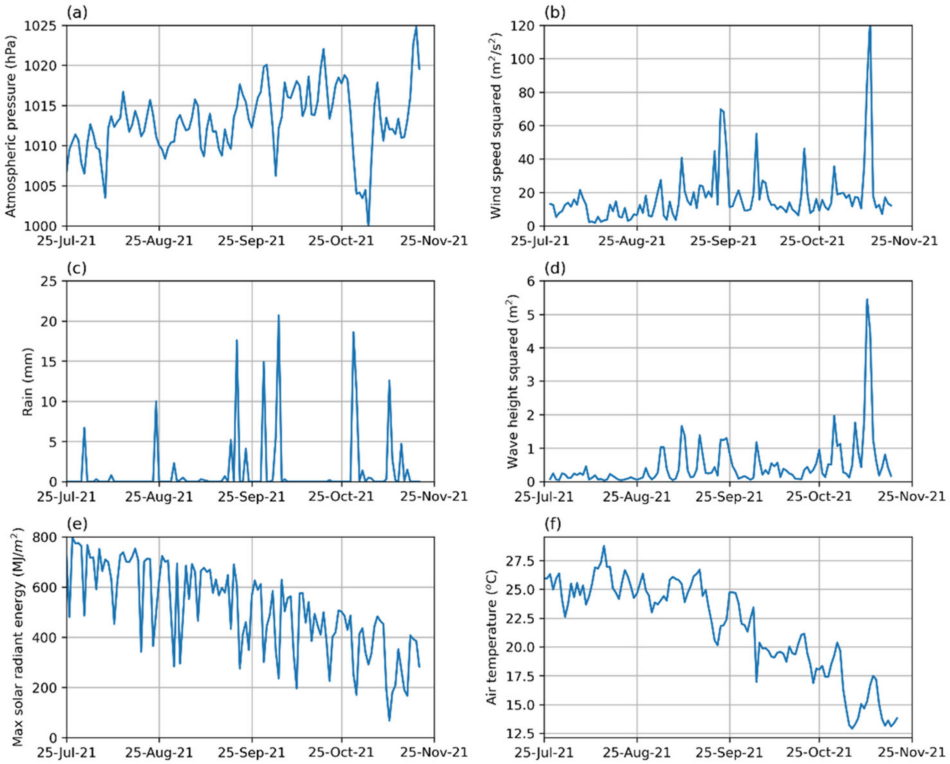

Figure 9. (**a**) Atmospheric pressure, (**b**) squared surface wind, (**c**) accumulated daily rainfall, (**d**) squared significant-wave height, (**e**) maximum daily solar radiation, and (**f**) surface air temperature.

Figure 9 also shows several variables that illustrate the meteorological forcing over the coastal ocean. Figure 9a presents the atmospheric pressure, with fairly stable values between 1007 and 1020 hPa, except for a minimum during the first days of November, which reached 1000 hPa. Figure 9e presents the maximum daily radiation, with a decreasing trend after the peak values in late July and intermittent minima that last one or two days and represent cloudy conditions. Figure 9c presents daily rainfall, with little rain during July and August and increasing in fall. High rainfall events correspond to periods of low radiation and high winds, except for the early-November period of low pressure that does not show wind intensification. Finally, Figure 9f shows the characteristics of the surface air

temperature, with maximum values until mid-September followed by a fast-decreasing trend, with some intermittency that is tallied to atmospheric pressure and solar radiation.

5. Results and Discussion

In order to illustrate the potential of the SPV for monitoring the inner shelf, in Figure 10 we present the evolution of the temperature distribution in the water column as obtained with the TD profiler during the field campaigns, carried out roughly about once per week between 28 July and 18 November (Table 4). In these profiles, we have removed the upper few meters of the water column such as to remove the temperature variations associated with the diurnal cycle.

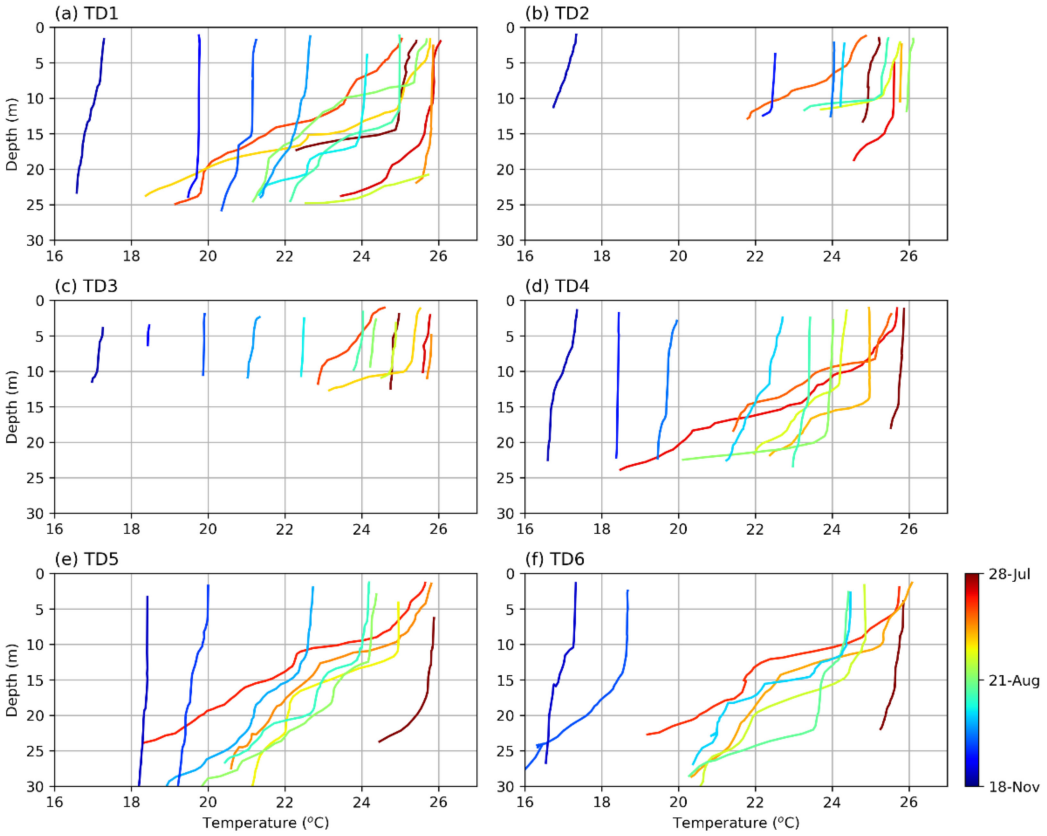

Figure 10. Temperature profiles (**a**–**f**) are colored as a function of time. Note that the start and end dates for stations (**a**–**c**) (top color bar) are not the same as for stations (**d**–**f**) (bottom color bar). The reader is referred to Table 4 for the exact sampling dates.

Stations TD2 and TD3 correspond to nearshore and relatively shallow waters (depths of 12 m and 11 m, respectively), which are fully affected by the influence of the surface gravity waves. For the short waves that characterize the nearshore platform off Barcelona, with typical periods of 4 s, waves feel the seafloor at water depths less than about 25 m. It is remarkable that some samples of these points exceed the depths of 12 m and 11 m. The sea floor in this area is irregular and the SPV is a floating device, so that it is difficult to sample the same exact location each time. The temperature profiles in TD2 and TD3 show that, during August and September, the upper 10 m of the water column remained most of the time over 24 °C and nearly homogeneous. The single exception is the August 17 profile (light red), which does show a clear thermocline, reflecting that sampling took place at a time of very low winds and waves, high solar radiation and maximum air temperature (Figure 9b,d,e,f). One relevant issue is that there are substantial differences between the temperature in these two sites, despite them being separated by only about 500 m, perhaps related to the location of TD2 just in front of a city runoff-water outlet. In particular, TD3

illustrates a gradual cooling of the water column throughout October and November as a result of the continuous decrease in solar radiation (Figure 9e).

At the deeper stations (TD1, TD4 and particularly TD5 and TD6) there is a substantial vertical structure except during late October and November. As at the shallower stations, the peak sea-surface temperatures take place in July and August and the temperatures progressively decrease during October and November. Station TD5 illustrates that the bottom waters (about 30 m) remain between about 18 and 21 °C during the entire period.

Rain events in excess of 10 mm per day occurred on 24 August, 20 and 28 September, 2 and 29 October, and 10 November. These rain events brought some runoff water from the city outlets but their effect was very limited to the surface of most waters. Finally, solar radiation was intermittent, caused by some cloudiness and rain, but until the end of September it remained nearly always above 400 Watts m^{-2}. Hence, we may infer that the observed decrease in sea-surface temperature was due to the negative trend in radiation and the air temperature drop rather than to the intermittent cloudiness.

One main mechanism for air–sea heat exchange is the flux of latent heat, which is proportional to water–air temperature difference near the sea surface. To analyze the water–air temperature difference during the period under study, we use daily-mean air temperatures as calculated from the hourly values provided by the Catalan Meteorological Service [24], and the SST values as derived from a combination of the TD near-surface data and the Sentinel-3 data flagged as excellent quality. With this strategy, we have produced a fairly continuous time series (values every few days) for daily temperature differences at the water–air interface (Figure 11). We are aware that the combination of the TD near-surface data and the satellite can introduce some unresolved daily variability, as the Sentinel data likely does not properly resolve the diurnal cycle. Nevertheless, Figure 11 shows that this strategy allows for resolving the autumn trend of increasing temperature differences.

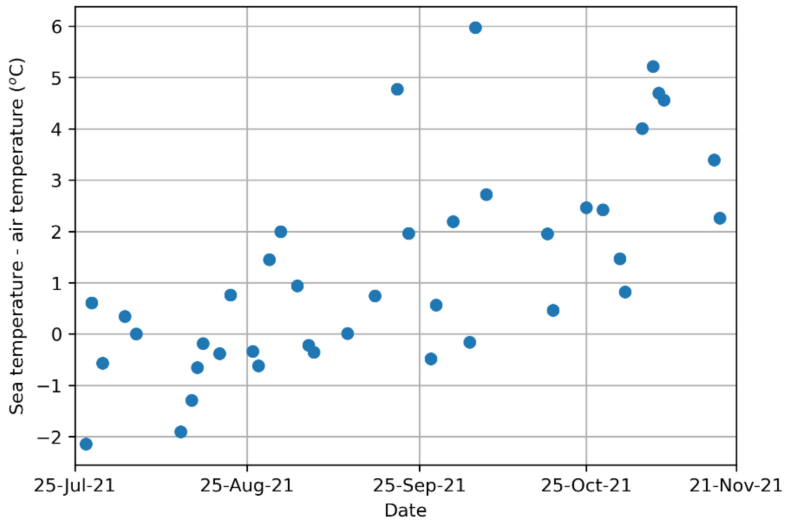

Figure 11. Time series of sea-surface water–air temperature differences in the study area.

The water–air temperature-difference time series also shows that there were three events of maximum differences, on 22 September, 5 October and 10 November (Figure 11), which correspond to windy and cloudy conditions that brought a substantial decrease in the surface air temperature while the surface waters remained much less affected (Figure 9b,e,f).

We close this article with a simple analysis of the TD data that shows the evolution of the water column and its relation with meteorological forcing, hence illustrating the SPV possibilities for monitoring the coastal ocean. We restrict our analysis to those stations with bottom depths of 20 m or greater, i.e., stations TD1 and TD4 close to shore and stations TD5 and TD6 further offshore (Table 3 and Figure 8).

For our purposes, we define two additional variables: the overall temperature gradient $\Delta T/\Delta z$, simply calculated as the temperature difference between the surface and bottom

waters divided by the water depth, and the (surface) mixed layer depth d, defined with a simple criterion that sets the base of the mixed layer where the temperature gradient exceeds 0.15 °C m^{-1} (which considers the accuracy of our temperature sensor, 0.1 °C) These two variables are useful to discuss some of the key mechanical and thermodynamic aspects in the evolution of the mixed layer depth.

The overall temperature gradient and the mixed-layer depth are inversely related. The surface mixed layer deepens through the entrainment of subsurface cold waters, which leads to a decrease in the overall temperature gradient. Both variables are also subject to changes in air–sea heat exchange, directly through changes in solar radiation or indirectly through an increase in the water–air temperature difference that enhances the latent and sensible heat fluxes.

The incorporation of subsurface waters into the surface mixed layer causes an increase in the potential energy of the water column that requires a source of kinetic energy, which has to come from wind- and wave-induced turbulence. Hence, we expect that there will be an inverse relation between mixed-layer depth and overall temperature gradient, and that both $\Delta T/\Delta z$ and d will respond to changes in the mechanical stirring (by waves, winds or both) but conditioned (possibly to a lesser degree) by variations in the ocean–atmosphere heat exchange.

In order to assess these relations, we present scattered plots of these two oceanographic variables ($\Delta T/\Delta z$ and d) as a function of three variables that represent the different types of daily-mean meteorological forcing: water–air temperature difference ΔT, squared significant wave-height $h_s{}^2$ and squared wind-speed W^2 (Figure 12).

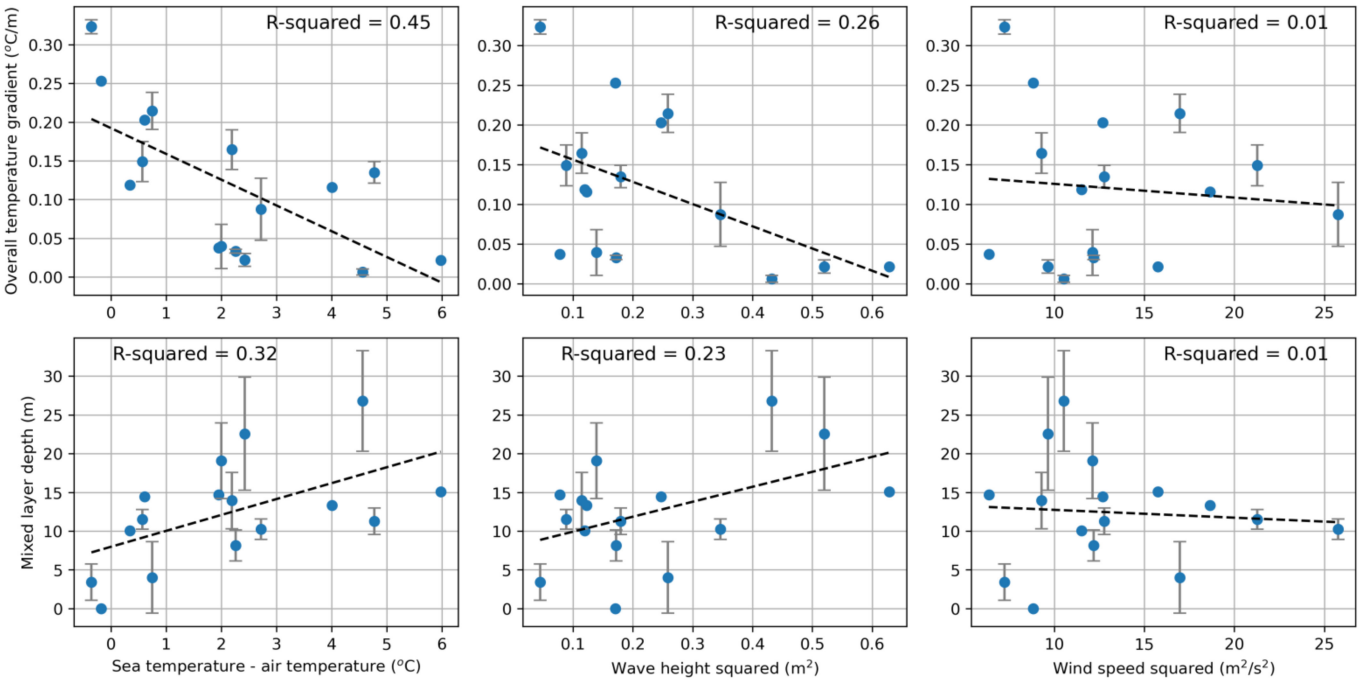

Figure 12. Scattered plots of (top panels) overall temperature gradient and (bottom panels) mixed-layer depth as a function of (from left to right) sea–air temperature difference, squared significant wave-height and squared wind-speed. The correlation coefficients are shown.

We observe that $\Delta T/\Delta z$ is inversely correlated to ΔT and d is directly correlated to ΔT (Figure 12, left panels). This is consistent with d increasing through the entrainment of subsurface waters into the mixed layer, hence causing a decrease in $\Delta T/\Delta z$.

Finally, we may explore if the energy required for vertical mixing comes from wave- or wind-induced turbulence, or both; notice that unstable vertical convection does not take place during summer-fall because the water column is stable as a result of the large increase in temperature towards the sea surface (Figure 10) [15]. We perform this analysis

with scattered plots of $\Delta T/\Delta z$ and d as a function of ${h_s}^2$ and W^2 (Figure 12, center and right panels), and find that there are significant linear correlations for the wave energy while the relation is not significant for the wind energy. Hence, we are left with the conclusion that the seasonal deepening of the surface mixed layer, and consequent reduction in the overall temperature gradient, is caused by the progressive increase in the wave field (Figure 9d). This result is consistent with the homogeneity of the water column in shallow locations, where the bottom depth is less than the vertical influence of the wave regime (except for summer periods when there was little wave activity). Further, the lack of correlation of $\Delta T/\Delta z$ and d with W^2 tells us that those waves driving mixing are largely non-locally generated. These results, which are consistent with observations in the inner shelf of other shelf regions [26], illustrate the good potential of data gathered with the SPV.

6. Conclusions

We have presented the development of a low-cost sampling strategy for coastal waters with the patí a vela (PV), a sustainable historical Catalan sailboat. The strategy is based on the incorporation of both a multiparametric box for sampling surface waters and a profiler for measuring the structure of the water column, in both cases with low-cost sensors and open-source data logging, turning the PV into a scientific PV (SPV).

We have enumerated the main components of the multiparametric box (temperature and salinity sensors in its first phase) and have thoroughly described the depth profiler (temperature in this initial stage). Further, we have also shown that the proposed sampling setup is fully compatible with the standard sailing of this sailboat, and the good performance of the TD low-cost sensors was confirmed through a favorable comparison with a commercial instrument.

The two different types of low-cost open-source instruments, the multiparametric box and the depth profiler, complement each other finely, in a sense replicating the standard sampling strategy of research vessels. In the multiparametric box, surface water is continuously pumped through the sensors allowing for a swift sampling of the sea-surface conditions along the path of the sailboat. With one or a few SPV, the surface waters of a fairly large area (10–50 km^2) can be sampled in relatively short times (just a few hours); this is very appropriate for monitoring the water quality of surface waters, particularly after periods of intense rain and water runoff from the city. The depth profiler is the necessary counterpart for sampling the structure of the water column, particularly useful for assessing temporal changes associated with both natural and anthropogenic forcing.

As an example of the potential of the SPV, we have presented and analyzed the results obtained through 15 one-day campaigns that used a temperature-depth (TD) profiler, carried out between July and November 2021 in as many as six stations within an area of about 3 km $\times$ 3 km, in water depths from the coastline to about 40 m. The temperature-depth profiles show that the mixed-layer depth increases and the overall temperature depth-gradient decreases from summer into fall as the height of non-local waves progressively increases and the air temperature decreases.

The scientific patí a vela (SPV) turns out to be an inexpensive and maneuverable oceanographic platform to sample the coastal waters, used either individually for regular monitoring or with several units installed in a small fleet aimed at investigating the spatiotemporal ocean variability. Because of its wide utilization, as a very versatile and inexpensive sailboat, the SPV can grow as an inclusive and collaborative citizen science platform that can effectively contribute towards an improved monitoring and understanding of the inner continental shelf, particularly near densely populated areas.

Author Contributions: Conceptualization, J.L.P. and I.O.; data collection, mostly O.C.; data analyses, I.O. and I.V.-C.; software, R.B., I.V.-C. and N.H.; methodology, validation, formal analysis, investigation, writing, M.C.-S., J.M., R.B., A.C., R.F., O.C., N.H., J.P. (Jaume Piera), J.S., C.S., I.V.-C., J.P. (Joan Puigdefabregas), I.O. and J.L.P.; funding acquisition, J.L.P. All authors have read and agreed to the published version of the manuscript.

Funding: This work has been carried out within the framework of the 2019 Barcelona Pla de Ciència, with funding from the Barcelona City Council through the project "Development of a citizen monitoring program for the Barcelona coastal waters: the Scientific Patí Vela" (PATI CIENTIFIC; references 19SO1645-006, 19SO1649-006, 19SO1651-006).

Institutional Review Board Statement: Not applicable.

Informed Consent Statement: Not applicable.

Data Availability Statement: Data supporting reported results can be found at https://paticientific.org/index.php/dades/ (accessed on 13 April 2022) and through https://zenodo.org/search (accessed on 13 April 2022) by searching "pati cientific".

Acknowledgments: We are thankful to all the staff and members of the CPVB for their continuous support in the SPV operations, and to Josep Pascual for his key help in the sensor validation exercise. We are very grateful to the Barcelona City Council for their support through projects PATÍ CIENTIFIC (Pla Barcelona Ciència 2019, ref. 19SO1645-006, 19SO1649-006, 19SO1651-006) and AULAMAR (Fundació Bit Habitat, ref. ID253). This article is a publication of the Unidad Océano y Clima of the Universidad de Las Palmas de Gran Canaria, a R+D+I CSIC-associate unit. R.B. is supported by the project EMSO—Laboratorios Submarinos Profundos. The ICM authors also recognize the institutional support of the Spanish Government through the Severo Ochoa Center of Excellence accreditation (CEX2019-000928-S).

Conflicts of Interest: The authors declare no conflict of interest.

References

1. Harley, C.D.G.; Hughes, A.R.; Hultgreen, K.M.; Miner, B.G.; Sorte, C.J.B.; Thornber, C.S.; Rodriguez, L.F.; Tomanek, L.; Williams, S.L. The impacts of climate change in coastal marine systems. *Ecol. Lett.* **2006**, *9*, 228–241. [CrossRef] [PubMed]
2. Amores, A.; Marcos, M.; Carrió, D.S.; Gómez-Pujol, L.L. Coastal Impacts of Storm Gloria (January 2020) over the Northwestern Mediteranean. *Nat. Hazards Earth Syst. Sci.* **2020**, *20*, 1955–1968. [CrossRef]
3. Alverson, K.; Baker, D.J. Taking the pulse of the oceans. *Science* **2006**, *314*, 1657. [CrossRef] [PubMed]
4. Brewin, R.J.W.; Hyder, K.; Andersson, A.J.; Billson, O.; Bresnahan, P.J.; Brewin, T.G.; Cyronak, T.; Dall'Olmo, G.; de Mora, L.; Graham, G.; et al. Expanding aquatic observations through recreation. *Front. Mar. Sci.* **2017**, *4*, 351. [CrossRef]
5. Brewin, R.J.W.; de Mora, L.; Jackson, T.; Brewin, T.G.; Shutler, J. On the Potential of Surfers to Monitor Environmental Indicadtors in The Coastal Zone. *PLoS ONE* **2015**, *10*, e0127706. [CrossRef] [PubMed]
6. Wright, S.; Hull, T.; Sivyer, D.B.; Pearce, D.; Pinnegar, J.K.; Sayer, M.D.J.; Mogg, A.O.M.; Azzopardi, E.; Gontarek, S.; Hyder, K. SCUBA divers as oceanographic samplers: The potential of dive computers to augment aquatic temperature monitoring. *Sci. Rep.* **2016**, *6*, 30164. [CrossRef] [PubMed]
7. Bresnahan, P.J.; Wirth, T.; Martz, T.R.; Andersson, A.J.; Cyronak, T.; D'Angelo, S.; Pennise, J.; Melville, W.K.; Lenain, L.; Statom, N. A sensor package for mapping pH and oxygen from mobile platforms. *Methods Oceanogr.* **2016**, *17*, 1–13. [CrossRef]
8. ACA. Quality of the Beaches and Swimming Areas of Catalonia. Available online: https://aplicacions.aca.gencat.cat/platgescat2/app.php/en/playa/157# (accessed on 21 October 2021).
9. BCN, Bany i Platges, Ajuntament de Barcelona. Available online: https://www.barcelona.cat/ca/que-pots-fer-a-bcn/banys-i-platges (accessed on 1 August 2019).
10. ICM, Estació Litoral de Barcelona, Institut de Ciències del Mar. Available online: http://coo.icm.csic.es/site-page/stations#Barcelona-ELB (accessed on 1 August 2019).
11. ICM, PUDEM SOS Application, Institut de Ciències del Mar. Available online: http://ide.cmima.csic.es/sos-js/web/examples/sos-apptest (accessed on 1 August 2019).
12. ICM. Oceanographic Data - Coastal Ocean Observatory. Available online: http://coo.icm.csic.es/site-page/oceanographic-data (accessed on 21 October 2021).
13. Arin, L.; Guillén, J.; Segura-Noguera, M.; Estrada, M. Open sea hydrographic forcing of nutrient and phytoplankton dynamics in a Med. coastal ecosystem. *Est. Coastal Shelf Sci.* **2013**, *133*, 116–128. [CrossRef]
14. Romero, E.; Peters, F.; Arin, L.; Guillén, J. Decreased seasonality and high variability of coastal plankton dynamics in an urban location of the NW Mediterranean. *J. Sea Res.* **2014**, *88*, 130–143. [CrossRef]
15. Guillén, J.; Arin, L.; Salat, J.; Puig, P.; Estrada, M.; Palanques, A.; Simarro, G.; Pascual, J. Coastal oceanographic signatures of heat waves and extreme events of dense water formation during the period 2002–2012 (Barcelona, NW Mediterranean). *Scientia Marina* **2018**, *82*, 189–206. [CrossRef]
16. ADIPAV. Reglamento de la Disciplina Patín a Vela. *Clase: Patín a Vela.* Available online: http://adipav.org/node/1503 (accessed on 31 January 2022).
17. Depoorter, G. *El Patín a Vela*; Editorial Hispano Europea: Sitges, Spain, 1974; p. 328.

18. Ortigosa, I.; Castells-Sanabra, M.; Llevadot, J.M.; Bardaji, R.; Hoareau, N.; Simon, C.; Pelegrí, J.; Casanova, I.V. Adapting the existing coastal Patí a vela fleet for scientific purposes. *J. Maritime Res.* **2020**, *17*, 88–94.
19. Beddows, P.A.; Mallon, E.K. Cave Pearl Data Logger: A Flexible Arduino-Based Logging Platform for Long-Term Monitoring in Harsh Environments. *Sensors* **2018**, *18*, 530. [CrossRef] [PubMed]
20. SeaDataNet. Quality Quality Control Procedures. &th Framework of Ec Dg Research, V2.0, May 2010. Available online: https://www.seadatanet.org/content/download/596/3118/file/SeaDataNet_QC_procedures_V2_(May_2010).pdf (accessed on 20 November 2021).
21. Software Manual Seasoft V2: SBE Data Processing. CTD Data Processing & Plotting Software for Windows. Sea-Bird Scientific. Available online: https://www.seabird.com/asset-get.download.jsa?code=251446 (accessed on 9 December 2017).
22. Grifoll, M.; Aretxabaleta, A.; Espino, M.; Warner, J. Along-shelf current variability on the Catalan inner-self (NW Mediterranean). *J. Geophys. Res.* **2012**, *117*, c09027. [CrossRef]
23. Gómez, M.J.C. Carretero. Wave Forecasting at the Spanish Coasts. *J. Atm. Ocean Sci.* **2005**, *10*, 389–405. [CrossRef]
24. Measurements of the Meteorological Stations of the City of Barcelona, Open Data BCN, Servei Meteorològic de Catalunya. Available online: https://opendata-ajuntament.barcelona.cat/data/ca/dataset/mesures-estacions-meteorologiques (accessed on 20 November 2021).
25. Sentinel 3, EUMETSAT. Dedicated Copernicus Satellite Mission Delivering a Variety of High-Quality Ocean Measurements. Available online: https://www.eumetsat.int/sentinel-3 (accessed on 20 November 2021).
26. Babanin, A.V. *Breaking and Dissipation of Ocean Surface Waves*; Cambridge Univ. Press: Cambridge, UK, 2011.